CARBON NANO-INK COATED OPEN CELL POLYURETHANE FOAM WITH MICRO-ARCHITECTURED MULTILAYER SKELETON FOR DAMPING APPLICATIONS

Xiao-Chong Zhang[a], Fabrizio Scarpa[ab]*, Ronan McHale[c], Andrew P. Limmack[a], Hua-Xin Peng[d]*

[a.] Advanced Composites Centre for Science and Innovation (ACCIS), Department of Aerospace Engineering, University of Bristol, Queen's Building, Bristol, BS8 1TR, United Kingdom.

[b.] Centre for Nanoscience and Quantum Information (NSQI), Tyndall Avenue, Bristol, BS8 1FD, United Kingdom.

[c.] Thomas Swan & Co. Ltd., Rotary Way, Consett, County Durham, DH8 7ND, United Kingdom

[d.] Institute for Composites Science Innovation (InCSI), School of Materials Science and Engineering, Zhejiang University, Hangzhou, 310027, PR China

*Corresponding authors. Email: f.scarpa@bristol.ac.uk (Fabrizio Scarpa), hxpengwork@zju.edu.cn (Hua-Xin Peng)

ABSTRACT

This work presents a novel complex microarchitectured foam material via multilayer nano-inks that provide a substantial improvement of the mechanical, energy absorption and dielectric performance in pristine open cell foams. A multilayer carbon nano-ink containing –COOH functionalised multi-walled carbon nanotubes are produced and used to dip-coat pristine polyurethane open cell foam structures with the assistance of a silane coupling agent. Another layer of water-based polyurethane dispersion is coated on top of the MWCNT layer coated foam to transform the single foam ribs in multilayer structures. The nano-ink dipping and drying process developed in this work creates a porous MWCNT layer with a fairly high MWNT content that covers the foam ribs. These carbon nanotube multi-layer coated foams show a significant energy absorption performance, with loss modulus and loss factors 165% and 100% higher than those from high-dissipation nano-foams fabricated by conventional foaming techniques and auxetic phase transformation respectively. These nano-ink multilayer coated foams with only one layer also exhibit an increase in electrical conductivity by a factor of two compared to other existing nano-ink coated open cell foams with a substantial higher number of layers (20).

Key words: Carbon nanoink; nano coating; energy absorption; nanocomposites foam.

1. Introduction

Polymer nanocomposite foams have received increasing attention in recent years due to their significantly improved multifunctional performance. These particular subset of foams exhibit increased strength [1-3], electrical conductivities [2, 4, 5], and damping [6-9] over their traditional counterparts. While the applications of polymer nanocomposite foams like flexible sensors [10] and electromagnetic shielding [2, 11] have been widely reported, very few studies have however focused on the damping applications for noise and vibration control. In recent years experimental studies and numerical modelling have been carried out to describe the widely reported interfacial sliding mechanism in nanocomposites for damping treatments. In the classical polymer/carbon nanotube (CNT) composite with nanoparticles embedded in the polymer matrix, the three interface couplings that induce energy dissipation are the polymer-nanotube, the nanotube-nanotube interfacial sliding, and the coaxial sliding of the tube walls within the multiwall carbon nanotube (MWNT) [12]. Polymer-nanotube sliding is determined by the CNT/polymer interfacial bonding and dispersion quality [13, 14], whereas nanotube-nanotube sliding within entangled CNTs is closely related to the filler content. The coaxial internal sliding between tube walls does not generate an appreciable increment in loss factor, however it has been shown to decrease the strain level threshold for which stick-slip dissipation occurs [15]. Most of the nanocomposites foams described in open literature have been produced by direct foaming, with the nanofillers being embedded inside the polymer skeleton. In that sense this type of microstructure makes use of the polymer-nanotube interfacial sliding to improve the overall damping performance. Verdejo and co-workers have added 0.1wt% MWNTs into flexible polyurethane (PU) foams, and managed to increase the sound absorption coefficient peak by 30% in the 1 kHz-2kHz frequency range compared with pristine PU foams [6]. The reason for this significant increase in acoustic absorption was attributed solely to the polymer-nanotube 'stick-slip' mechanism with increased cell sizes. Bandarian et al [9] compared the loss factor (tan δ) and sound absorption coefficient of carboxyl, hydroxyl and amide functionalised MWNTs (0.1wt%) modified open cell PU foam. In agreement with what observed by Verdejo et al, Bandarian and co-workers also witnessed an increase of the sound absorption peak of the foam between 1 kHz- 2 kHz. The improvement of the mechanical and acoustic damping in the PU/CNT-COOH and PU/CNT-OH foams was however attributed to the micro voids structure produced by gas during the

reaction between the functional groups on the CNT surfaces and the isocyanate. The foam with amide functionalized CNTs showed however a decrement in loss factor caused by the strong covalent bonds which inhibited the polymer-nanotube 'stick-slip' mechanism [9]. Polymer foams with high CNT content tend also to not exhibit a homogeneous dispersion of nanoparticles, which leads to a deterioration of the mechanical properties. For example, Liang et al.[16] have developed soy-based PU foams reinforced with varying weight fractions of MWNTs. While the flexural modulus and strength increased by ~30% by using 0.5wt% of embedded MWNT only, a further increment of MWNT content to 1wt% caused a sharp drop of those mechanical properties.

A region with high CNT content in the composite foam is required to make an efficient use of the nanotube-nanotube interfacial sliding mechanism. Nano-ink coatings applied to the cellular structure of an open cell foam can generate the type of microstructure able to provide enhancements to the damping performance. However, to the best of the Authors' knowledge very few studies have been performed with a conductive nanoink coating on polymer open cell foams. These studies have focused mainly on pressure sensitive sensing applications with a single layer of ink coating the foam skeleton [17], or infiltrating the foam cell [18]. No work has been published so far about the damping performance of nano-coated open cell foams making use of the nanotube-nanotube damping mechanism. Another aspect of novelty of this work is the development and use of multi-layer ink coating technique to generate highly entangled CNT network region on the foam skeleton by repeating a simple dip-coating process. The process creates cellular foams with individual strut having a multilayer micro-architecture where the MWNT ink layer represents a sandwich core and the polyurethane dispersion (PUD) coating acts as sealant layer. Foams containing 1 to 4 layers of MWNT coatings were analysed in view of their coating coverage, electrical conductivity and viscoelastic damping performance. The viscoelastic characterisation was performed following Dynamic Mechanical Analyser (DMA) techniques, while stiffness and energy absorption properties were determined by mechanical compressive quasi-static and cyclic tests.

2. Experimental

2.1 Nano-ink preparation

Carboxylic functionalised Elicarb® MWNT with over 70% purity, average diameter of 20 nm and 10's of microns in length were supplied by Thomas Swan Ltd, UK. Fig. 1 shows an

example of Transmission Electron Microscopy (TEM) images of these MWNTs. The as-received MWNTs were dried in a vacuum oven to remove moisture. Isopropanol alcohol (IPA) was used as solvent for the MWNT dispersion due to its relatively low surface tension of 21.4mN/m [19] at room temperature, compared with the analogous value of deionized water (72.75mN/m [20]). MWNTs were added directly into the IPA, followed by ultrasonication performed with a probe sonicator for 30 mins with the assistance of polyvinylpyrrolidone (PVP) as dispersant. An initial master batch of 0.3wt% solution was produced; the ink was diluted to the required wt% with additional isopropanol alcohol.

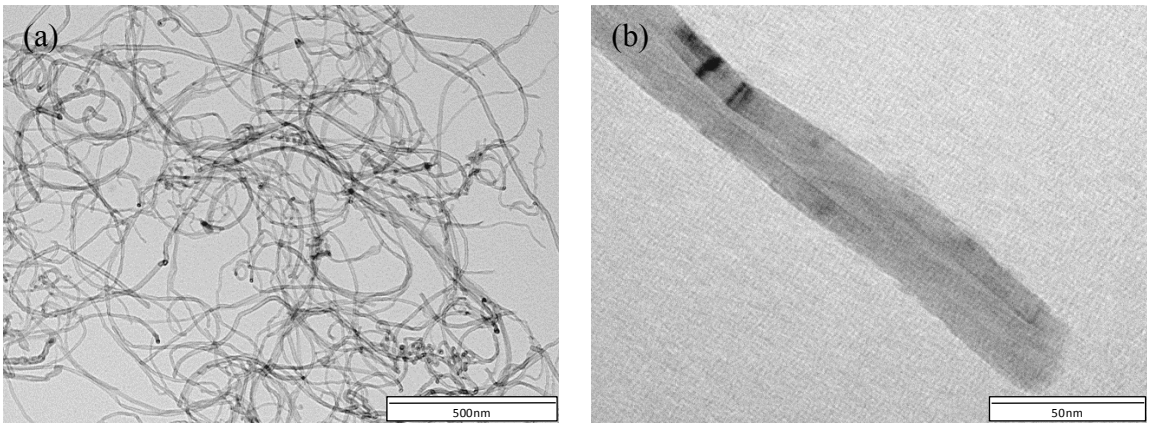

Fig. 1 TEM images of the MWNT-COOH (a) at ×50,000 magnification, and (b) under ×500,000 magnification.

2.2 Multilayer coating process

The first step of coating involves a silane treatment consisting in (3-Amin opropyl)triethoxysilane used as coupling agent for bonding the CNTs onto the foam struts. IPA with pH value of 3.5 was used to dilute the silane concentration to 0.5wt%. Pristine PU foam obtained from SM Upholstery Ltd. (density of 27kg/m^3, with 2047-2244 pores/m) was O2-plasma treated for 1 minute and then immediately immersed and agitated in the silane solution. Manual pressure was exerted to help soaking the solution faster. Before drying, the excessive solution was removed by leaving the foam on a 3M chemical sorbent sheet for 30min. The silane-treated foam was then dried at 80 °C for 4 hours.

In a second step the silane-treated foam was immersed into the MWNT ink. The infiltration of the ink into the foam cells was facilitated by agitating the foam samples. The foam was then removed from the ink after 20 mins, hand pressed and placed on an absorbent sheet to remove excessive material. After drying at 80 °C for 12 hours the nanoink-coated foam was removed from the oven for the top coating procedure.

We used a water-based aliphatic polyurethane dispersion (PUD) U4101 with solids content of 39-41 and elongation at break of 1400% [21] provided by Alberdingk Boley and used as top coating. This solution was used to seal the MWNT coating as a sandwich core between the base PU foam strut and PUD, as illustrated in Fig. 2. The foam was then dried in the oven for 5 hours at 50°C.

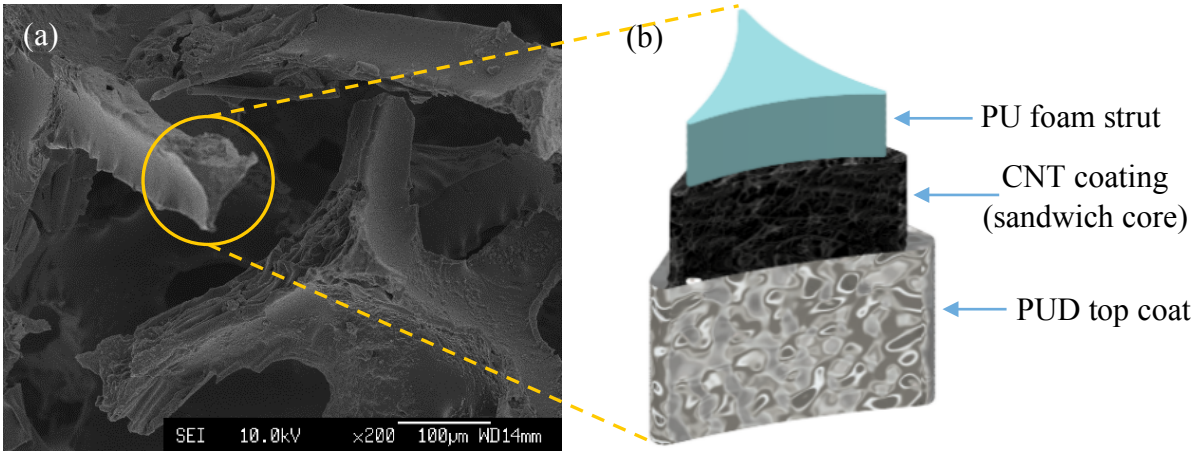

Fig. 2 SEM image of pristine PU foam strut (a) and, schematic of the coating formed strut sandwich structure (showing one layer of MWNT coating here) (b)

The surface coverage of foam strut by the MWNTs is a key factor that governs the damping performance. To make use of the CNT-CNT frictional slippage existing in multi-walled nanotubes the strut surface should preferably fully covered by the MWNTs ink coating. Therefore we produced one layer of MWNT ink coating with various ink concentrations (0.01wt%, 0.05wt%, 0.1wt%, 0.2wt%, and 0.3wt %) to evaluate the influence and type of surface coverage.

The coating process described above can be considered as the procedure necessary to produce one sandwich-type layer coating. By repeating the same procedure 1 to 3 times and treating the PUD top coat as the next layer's base coat we could produce samples containing 1 to 4 layers of micro- architectured sandwich rib coating. Pristine and PUD coated foams without the MWNT ink ribs sandwich core were also fabricated and tested for control. Fig.3 shows the as-produced foams (200×300×400 mm^3) containing between zero and four layers of the

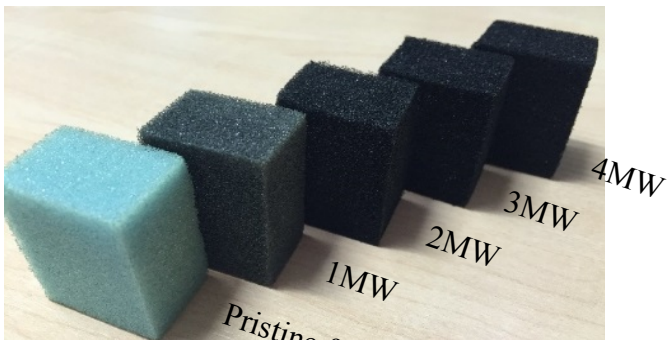

sandwich coating.

Fig. 3. As-produced samples with increasing number of MWNT layers (left to right).

2.3 Measurements

The conductivity of the foams coated with 0.01wt%~0.3wt% ink (without top coating) were measured by using a Keithley 2100 digital multimeter under two points measuring mode (ASTM D4496-04 standard). This test was only performed to verify the possible formation of conductive networks, and to determine therefore the coverage and uniformity of the ink coating on the surface. The actual MWNT content coated on the foam was measured by weighting the foams before and after the ink-coating process.

The amplitude, frequency and temperature dependency of the viscoelastic properties (storage modulus E', loss modulus E" and tanδ) of the multilayer-coated foams were evaluated by using a Dynamic Mechanical Analyser (DMA+/NUT/022/B-Metravib) under compression mode. The specimens were subjected to a sinusoidal dynamic strain varying from 0.2% to 2% at a fixed frequency of 10Hz at room temperature. Frequency scans of 1 Hz - 40Hz were then applied under a temperature sweep between 30°C and 130°C with 1% strain under a heating rate of 5°C/min. Both static and quasi-static compression-compression cyclic tests were performed at room temperature by using Shimadzu AGS X Series universal testing machine with 1KN load cell at crosshead speed of 5mm/min under stroke control with maximum stroke of 1.5mm (3.75 % of compressive strain) in 1Hz triangular waveform under room temperature and 36% humidity. The aim of these tests was to obtain an overall characterization on the static and cyclic performance of the various types of foams and provide a benchmark to the DMA data. An initial set of five cyclic loading at 1 Hz and room temperature was also performed to verify the mechanical stability of the sample. After the first cycles, the hysteresis curves and elastic modulus of the foams showed a robust stability. DSC measurements were performed on a TA Instruments Q100 Calorimeter in two scans. The first scan was to remove the thermal history of the samples, whereas the second scan was performed between -70 °C and 300 °C with a heating/cooling rate of 10°C/min. The identification of the transition temperature by the DSC measurements was performed following the ASTM D7426-08 standard. Five specimens from each sample batch were tested to acquire a statistical distribution of the results.

3. Results and discussions

3.1 Surface morphology and conductivity

The morphologies of the surfaces of the foam struts after the ink coating with various MWNT concentrations are shown in SEM images of Fig. 4. With increasing concentration of the MWNT inks one can observe a higher roughness of the skeleton surface (Figs. 4. a1, b1, c1, d1, and e1). The insets in these figures, together with the images shown in Figs. 4. a2, b2, c2, d2, and e2 feature the corresponding higher magnification pictures of the foam struts. No undispersed CNT bundles are observed in all images, something that proves that a uniform dispersion and deposition was achieved by using our technique. With relatively low MWNTs concentrations (0.01wt% and 0.05wt%) the ink-coated foam surface exhibits less entangled CNTs networks, and large uncoated surfaces can be also observed (Fig. 4. a2 and b2).

As the ink concentration increases a more pronounced deposition of MWNTs starts to appear on foam surface. The 0.1wt% (Fig.4. c2), 0.2wt% (Fig.4 d2) and 0.3wt% (Fig.4. e2) ink-coated surfaces all reveal similar morphologies, with the MWNTs bridging each other and forming highly entangled MWNTs networks. The morphologies of the MWNTs network distributions appear to be very similar both at the surface and internal regions of the foam (see the SEM images of the Supplementary File). This feature indicates that any non-uniform dip-coating effect due to the permeability of the foam was negligible, because the low surface tension of the IPA, large cells dimensions (~ 500 μm) and the small sample sizes made the infiltration process effective.

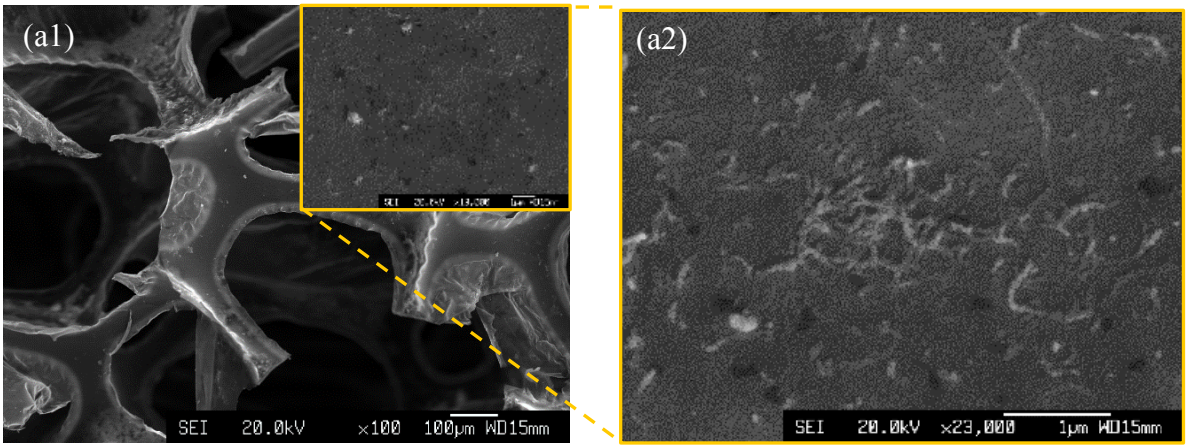

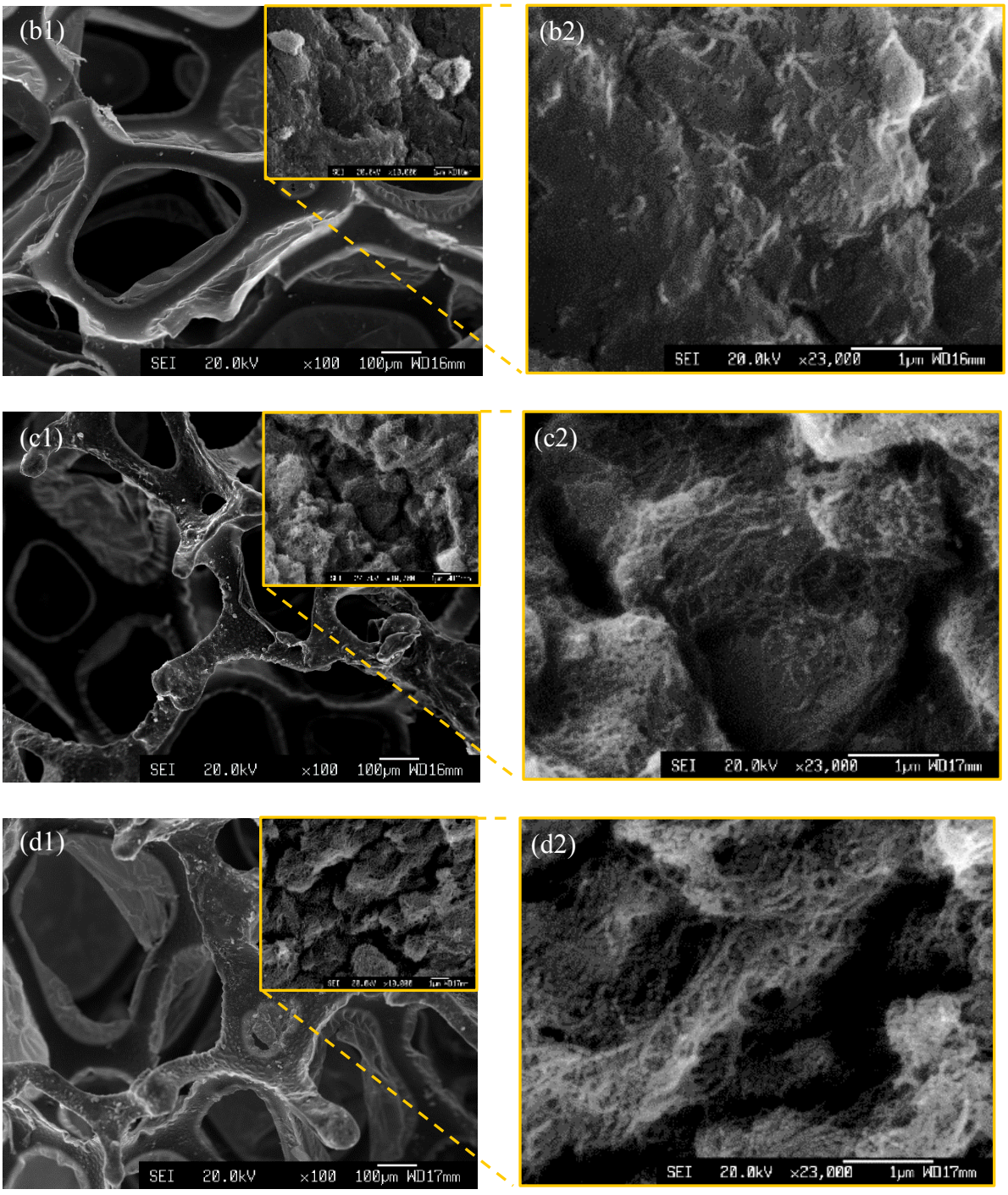
(b1)
SEI 20.0kV ×100 100μm WD16mm
(b2)
SEI 20.0kV ×23,000 1μm WD16mm
(c1)
SEI 20.0kV ×100 100μm WD16mm
(c2)
SEI 20.0kV ×23,000 1μm WD17mm
(d1)
SEI 20.0kV ×100 100μm WD17mm
(d2)
SEI 20.0kV ×23,000 1μm WD17mm

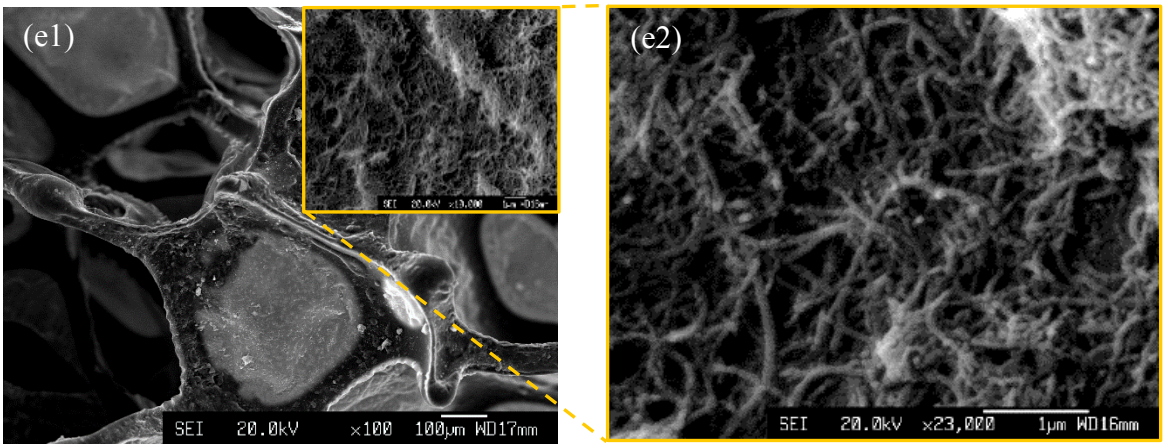

Fig. 4. SEM images of PU foam skeleton coated with MWNT ink with concentration of 0.01wt% (a1, 2), 0.05wt% (b1, 2), 0.1wt% (c1, 2), 0.2wt% (d1, 2), and 0.3wt% (e1, 2).

This surface morphology of the MWNT coating can be evinced by observing the foam electrical conductivity versus the actual weight percentage of the MWNT coated on the foam skeleton (Fig. 5). In agreement with observations from the SEM images, the percolation threshold region is between 0.05wt% and 0.1wt% of the ink concentration. At relatively high ink concentrations (0.1wt% 0.2wt% and 0.3wt% ink) the coated foam with well-developed MWNT conductive networks showed a conductivity of 1 S/m, ~1200% times higher than the one provided by the 0.05wt% ink coated foam samples. Chun et al[18] have applied graphene ink layers on PU foam and observed the presence of a foam conductivity of ~0.56 S/m with 30 layers of coating. The foam presented in our work features the double of that conductivity value, with only one coating layer and half of the ink concentration used in[18]. Instead of filling the foam cell with nanoparticles, our ink coating method requires a coating on the foam strut only, and significantly lower quantity of CNTs (half of the ink concentration) by making use of the entanglement of CNT networks.

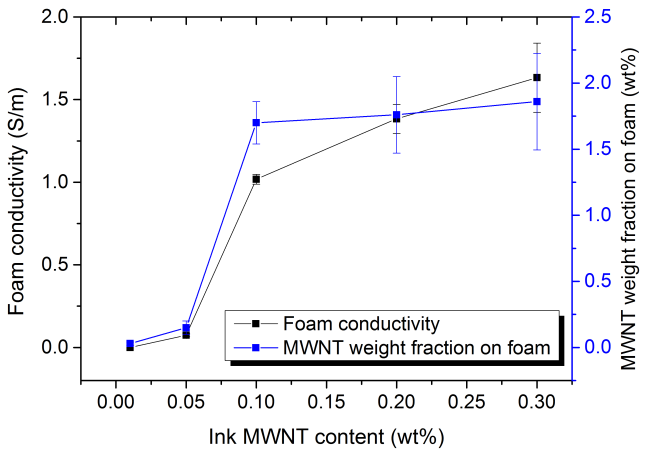

Fig. 5. One layer ink coated foam electrical conductivity and coating weight fraction versus ink concentration.

Due to the saturation of the surface coverage the electrical conductivity did not increase further by a significant amount, showing only a ~50% improvement when tripling the MWNT content from 0.1wt% to 0.3wt%. This surface coverage saturation is also proved by the plateau region in Fig. 5. It can be therefore concluded that the 0.1wt% MWNT ink was the most effective for the surface coverage of the foam skeleton, and was then adopted for the successive studies of the multilayer coating analysis.

3.2 Static and cyclic compression tests on the multilayer architectured foams

The results from the uniaxial compression test are shown in Fig.6. Both the MWNT ink layer and PUD layer foam samples showed a variation of the mechanical properties versus the pristine foam configurations. In order to analyse the mechanical performance outside the linear elastic range, we chose the stress at 10% strain as the one corresponding to the plateau stress (see Fig. 6a). To separate effects of the PUD layer, samples with one layer (1PUD) and four layers (4PUD) of PUD coating were tested for comparison purpose. As shown in Fig. 6, the pristine PU foam revealed the smallest elastic modulus (E) and a stress at 10% strain (σ_{10}) of 8.5KPa among the tested foams. On the contrary, the '2MW', '3MW', and '4MW' samples with increasing number of coatings showed a pronounced and gradual increase of both the elastic modulus and the stress at 10% of compressive strain. With four layers of MWNT coating, '4MW' exhibited a quite remarkable 220% and 190% increments of E and σ_{10} respectively, when compared against the analogous values of the pristine foam. The stiffening and strengthening effects of the proposed multilayer coating technique is much more effective than the one exhibited in samples made of the conventional foaming technique; Bandarian et al. [9] reported only a ~50% improvement in the foam tangent modulus with 0.1wt% MWNT-COOH embedded in PU foam. These significant improvements in the mechanical performance can be attributed to the strengthening effect of the PUD layer and the one provided by the MWNT core layer. By comparing the mechanical properties of the pristine foam and the '1PUD' and '4PUD' samples (Figs. 6a and b) one can conclude that the PUD layer can only improve the mechanical performance only to certain level (~50% increment in both E and σ_{10} with 1PUD). The embedding of further layers of PUD coatings did not exhibit any appreciable strengthening effect, and it is therefore reasonable to conclude that the observed improvement in the foams mechanical properties are mainly due to the presence of the MWNT core layer. The amino group on the silane coated foam reacted with

the carboxyl group on the MWNT surface forming a strong chemical bonding. The chemical group, together with the entangled MWNTs network structure shown in Fig. 4 formed a rigid sheath around the flexible PU foam skeleton, and contributed significantly to improve the mechanical performance of the porous material. The foam density increased with increasing number of coating layer, thus the specific modulus and stress shown in Fig 6 (c) did not show an apparent variation from '1MW' to '4MW'. Due to the light weight and high specific surface area of the CNTs '4MW' and '4PUD' revealed very similar densities but with distinct mechanical properties (Fig. 6(c)) with '4MW' showing ~90% higher elastic modulus, and ~80% higher stress at 10% strain than that of the '4PUD' sample, and thus the specific mechanical properties of '4MW' is outperforming '4PUD'. Verdejo et al.[6] have applied the foaming technique with up to 0.2wt% MWNTs embedded in the flexible PU foam skeleton and concluded that due to the variation in foam density and cellular structures the specific Young's modulus decreased with increasing CNT content. The ink coating technique used in this work provides a strengthening effect of the MWNT core layer in between the PU layers, thus preventing the variation in cell size caused by non-uniform foaming.

(a)

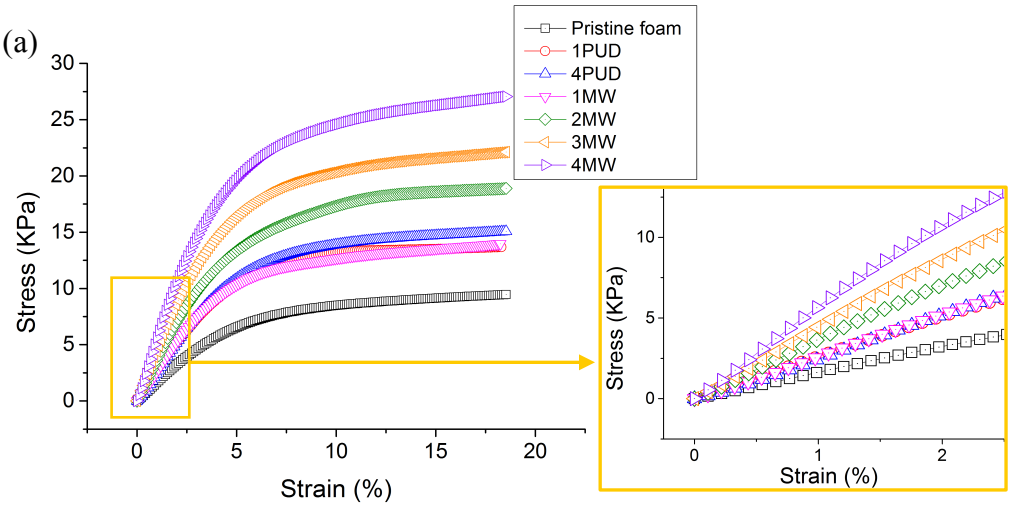

(b)

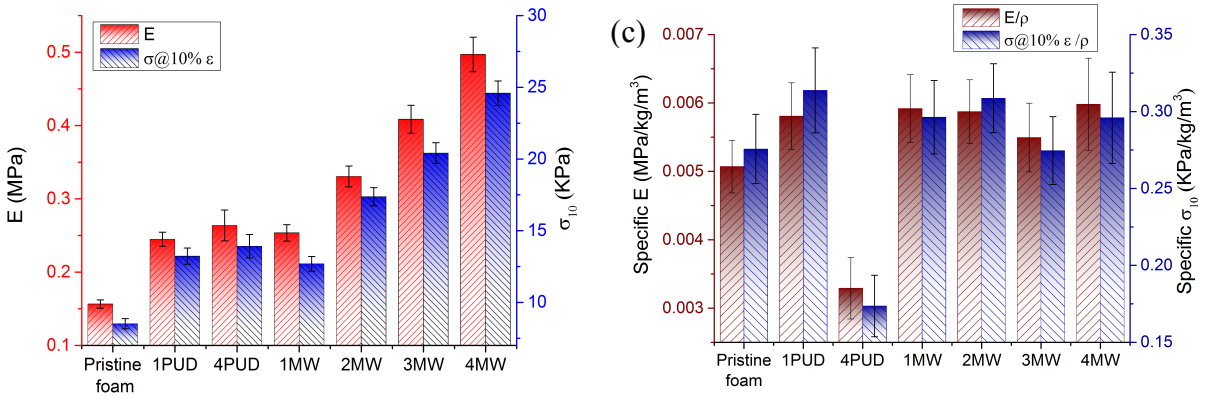

Fig. 6. Plot of single compression stress-strain curve (a), elastic modulus and stress at 10% strain (b), and specific modulus and specific stress at 10% strain (c) of multilayer coated foams.

Fig.7 shows the normalised energy dissipated in one loading-unloading cycle (ΔW) by foams in quasi-static tests and the corresponding loss factor (η) given by the following equation:

$$\eta = \frac{\Delta W}{U} \quad (1)$$

Where U is the maximum energy stored during a cycle and can be calculated from the area under the middle line of the hysteresis loop [22].

In Fig. 7 the dissipated energy ΔW for each coated foam configuration has been normalised against the analogous quantity related to the pristine foams. As shown in Fig.7 both the dissipated energy and the loss factor increased with increasing MWNT coating layers, when compared with the results from the baseline PU foam. The 4-layers MWNTs coated foams exhibited a ~380% increment in ΔW, with loss factors close to ~0.25. This value is 66% higher than the one of the pristine PU foam. Both the PUD layers and the MWNT core layers appeared to contribute to the observed improvements in the quasi-static and cyclic mechanical properties. By comparing the performance of the pristine foam and the '1PUD' '4PUD' and '4MW' porous configurations it is however possible to conclude that the presence of a PUD layer has only a limited effect in enhancing the damping performance. One layer of PUD coating provided an increase of ~80% of the energy dissipation compared with the baseline PU foam, but by adding 4 layers of PUD coating a further increment of only ~45% was obtained. On the opposite, the 4-layers MWNT coated samples (4MW) added another ~260% increment of ΔW on top of the one provided by the samples with four layers of PUD coating. It is apparent that this ~260% increase in energy dissipation can be solely attributed to the presence of the MWNT core layer, and proves the fact that the MWNT core

layer played a key role in the enhancement of the damping performance. It is also interesting to notice that the '1MW' sample showed a smaller ΔW normalised value than that the one exhibited by the 1PUD configuration that contained the same number of PUD layers, and was expected to exhibit a lower normalised energy dissipated. This fact could be explained by the strong chemical bonding existing between the MWNT-COOH, PU and PUD layer, together with the two types of damping mechanisms within the core layer itself, which will be discussed in the following paragraph.

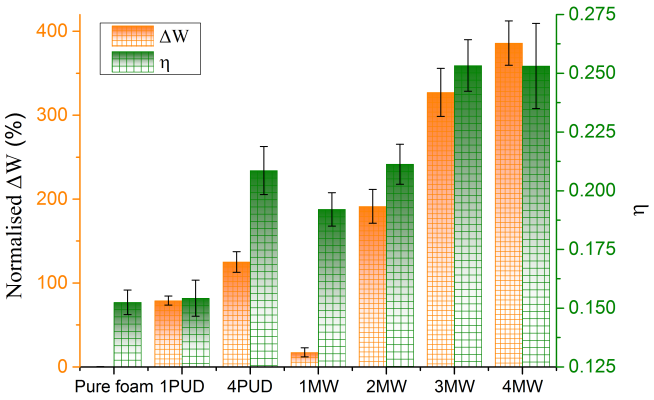

Fig.7. Normalised dissipated energy and loss factor of multilayer coated foams obtained from quasi-static cyclic compression tests.

3.3 Viscoelastic damping performance

The amplitude dependency of the viscoelastic properties (storage modulus E', loss modulus E") of the samples was evaluated by using a Dynamic Mechanical Analyser. Figs.8. (a), (b) and (c) show the storage modulus, loss modulus and loss factors of the tested specimens. The storage modulus E' (Fig.8 (a)) increased with the presence of increasing numbers of MWNT coating layers, which in agreement with the trend observed from the quasi-static cyclic tests (Fig. 6 (b)). However, the magnitude of the elastic modulus is higher than the one recorded for the storage modulus from the DMA test. One of the reasons is that the elastic modulus was calculated with strain up to 3% whereas the DMA only presented the dynamic strain up to 2%. Together with the differences in testing frequency and the input signal (sinusoidal for DMA, triangular for quasi-static test) which led to different level of energy input per cycle, it is difficult to find a corresponding relationship between the results obtained from these two tests [12, 23].

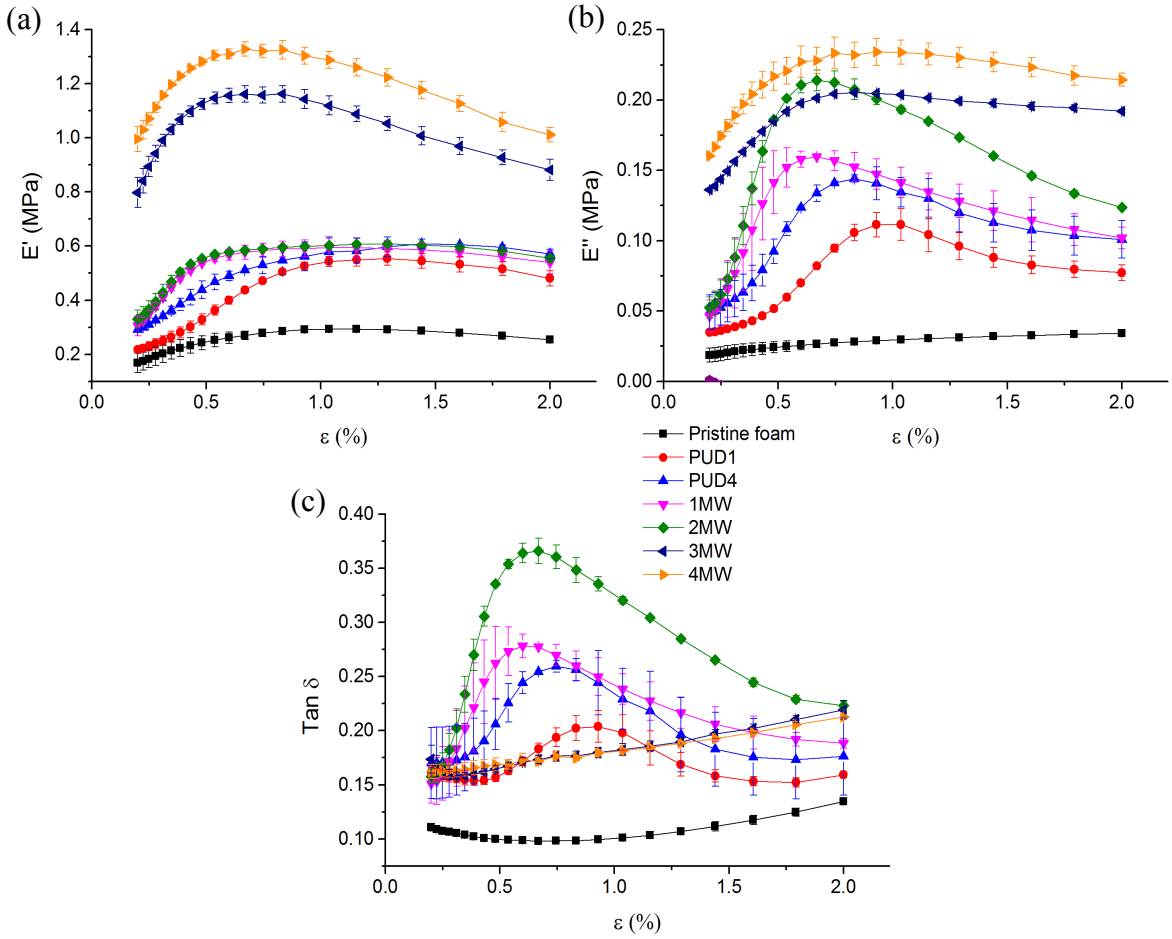

Fig. 8. Storage modulus (a), loss modulus (b), and loss factor (c) as a function of the dynamic strain obtained from DMA analysis.

Similarly with the results from the quasi-static cyclic loading tests, the loss modulus, increased with increasing numbers of MWNT coating layers (Fig.8 (b)). As discussed previously, both the PUD layers and the MWNT core contributed to this increment. Additionally, two possible damping mechanisms within the MWNT core layers could be further argued for. In a similar way to any conventional CNTs embedded in polymer matrix nanocomposites two main damping mechanisms exist in the MWNT core: the energy dissipation caused by (a) CNT-polymer interfacial sliding and (b) the energy dissipation caused by the CNT-CNT sliding [12]. Unlike conventional polymer based nanocomposites that are mainly characterised by the stick-slip mechanism at the CNT-polymer interface, the MWNT core contains more entangled CNTs that provide a larger CNT-CNT interface, and therefore would dissipate energy mainly through the CNT-CNT interfacial sliding. When considering the chemical bond formed by the –COOH functional group between the MWNTs and the PUDs, the CNT-polymer interface retains a much stronger bonding and therefore requires a higher critical shear strain (stress) to activate the CNT-polymer interfacial sliding

mechanism compared to the case of the interfacial sliding between CNTs [12]. Hence, as indicated in Fig. 8 (b), the sharp increment in loss modulus at lower dynamic strain is caused primarily by the CNT-CNT interfacial sliding mechanism. With the increase of the dynamic strain the other CNT-polymer energy dissipation mechanism started to contribute to the overall damping performance, reaching a peak of storage and loss modulus at a specific strain, with the two damping mechanism been fully activated. The position of the E" peak shifted to lower dynamic strains with increasing numbers of MWNT layers as indicated by the arrow in Fig.8 (b), this phenomenon likely caused by varying interface shear stresses between each ink layer. The samples coated by four MWNT layers revealed a ~660% increment in loss modulus compared with the one of the baseline PU foam.

The loss factor (tan δ) is plotted in Fig.8 (c). Although the samples containing between three and four layers of coating showed the higher loss modulus, their loss factor dropped in values close to the ones of the PUD coated sample due to their high storage modulus. The samples containing two layers of coating showed the highest loss factor (~0.37 at 0.66% strain), increased by 185% and 85% compared to the ones of the baseline PU and 1 PUD layer coated foams respectively. Such increment in loss factor by using the CNT-CNT frictional sliding is much more effective than the one present in foams that take advantage of the CNT-polymer matrix damping mechanism. For example, Bandarian[9] and co-workers have used the foaming technique with 0.1wt% COOH functionalised MWNTs embedded in the foam strut, and observed an increase of the loss factor by ~20% from 0.21 to 0.25 at 20°C. In our case, the ink-coated foam shows a 270% increment in loss factor for 1 wt% with 2 coating layers, which is however a higher weight fraction than the one used in [9]. Our in-coated foams appear to be also more effective in damping than high-energy dissipation auxetic foams; Bianchi [24] has observed that the damping capability of conventional open cell PU foams improves by transforming the same pristine foam used in this study into an auxetic phase, with the foam loss factor increased by 83% from 0.12 to 0.22 By applying the ink coating technique proposed in this work we have however achieved a further 100% increment in loss factor.

The viscoelastic properties of the ink coated foams were described in master curves (Fig.9) superposed using the Williams-Landel-Ferry model [25] with a reference temperature of 75°C. The data used for time-temperature superposition was selected according to the Cole-cole plot, which is a log-log plot of the loss modulus vs. storage modulus used to determine whether the tested material is thermodynamically simple [26]. These plots are considered a

standard in industry to evaluate the performance of the material outside the experimental limitations [27].

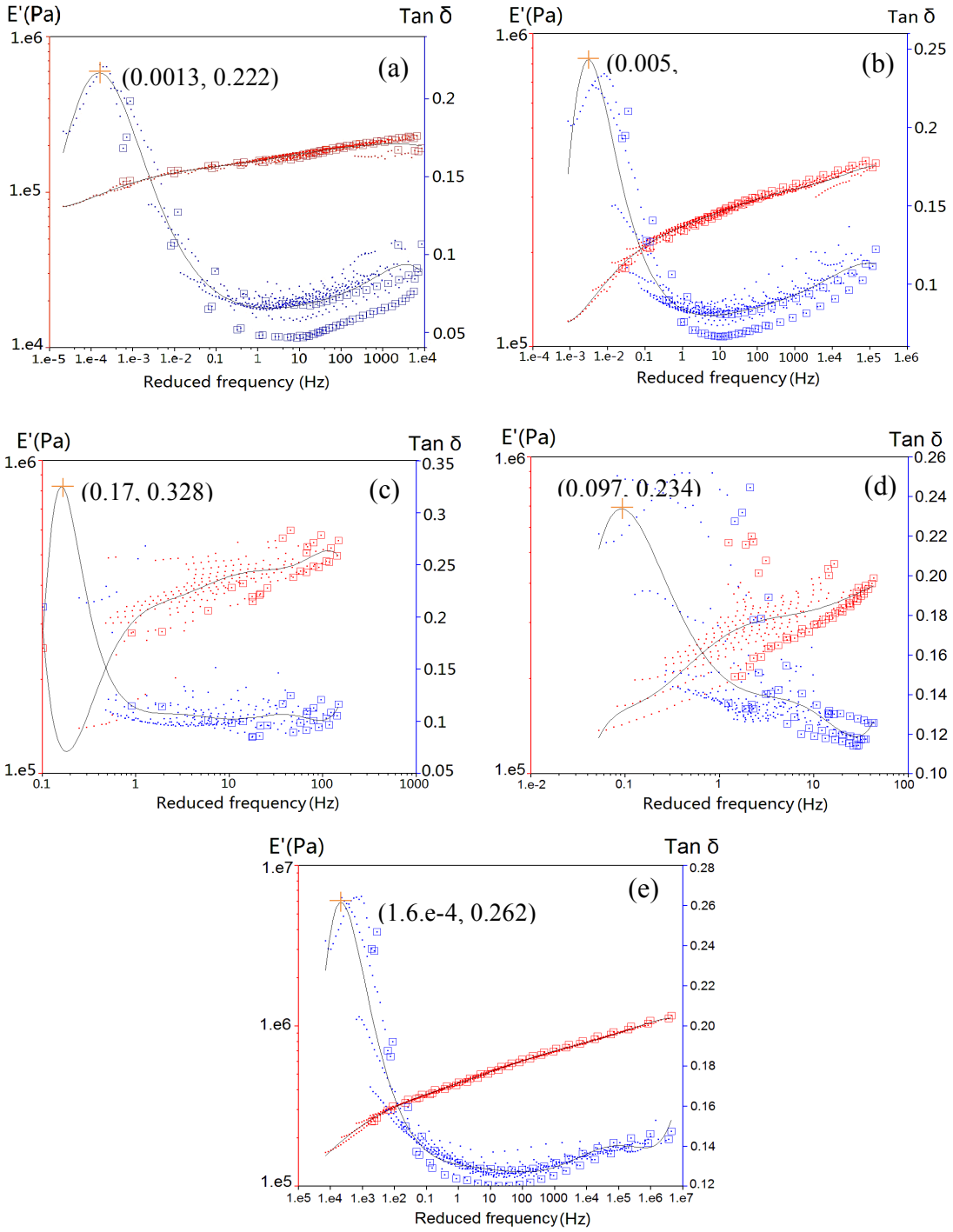

Fig. 9 Reduced frequency nomogram for pristine foam (a), 1MW (b), 2MW (c), 3MW (d), and 4MW (e).

The pristine foam, ('1MW'), and the '4MW' samples showed a relatively smooth fitting, whereas '2MW' and '3MW' showing scattered data points not aligned with the fitted curve which indicates that the assumptions of the WLF are not met. Containing 1 layer of coating

the ‘1MW’ sample exhibits the density almost the same as that of the pristine foam, allowing most of the air compressed out during the test, whereas the ‘2MW’ and ‘3MW’ foams contained increased skeleton thickness causing air trapped in the foam during cyclic compression, hence the sample cannot be considered as thermodynamically simple. With the number of coating layers further increased to four the nomogram of ‘4MW’ revealed a smooth fitting due to the stiffened continuous foam strut which made the foam exhibited a viscoelastic performance similar to a dense material. The greater uncertainties at the extreme upper and lower temperatures may have caused the mismatch [27] at lower and higher frequency of the nomogram.

The peak loss factor and the corresponding optimal reduced frequency for each specimen are indicated in the plots. The optimal reduced frequency increased with increasing numbers of the MWNT coating layers, dropping back to 1.6e-4 with four layers of coating. In agreement with what observed on the strain scan (Fig.8), the 2MW samples showed the highest values of loss factor, and the introduction of more coating layers resulted in a drop of the loss factors due to the increased storage modulus.

3.4 Thermal analysis

As shown in Fig. 10, no significant difference was observed between the various samples in terms of their second order transition temperatures. When heating the pristine foams from -70 °C a second phase transition was observed at -45°C, further heating affords no additional phase change until 114°C, where another second-order transition is observed. As the MWNTs are not embedded inside neither the pristine PU foam nor the PUD layer, the segmental mobility of the polymer chain was not restricted, thus the transition temperature stayed with increasing coating layers. With the increase of the temperature the exothermic peak of the pristine PU appeared at 270°C, whereas the samples ‘1PU’ and ‘4PU’ had the exothermic peak at around 220°C. This difference was caused by the PUD layer that has a lower decomposition temperature than the one of the baseline PU foam. The anoxic exothermal resulted from the recombination of the molecular fragments into lower energy oligomers which transported into gas phase [28], resulting in the presence of an endothermic peak.

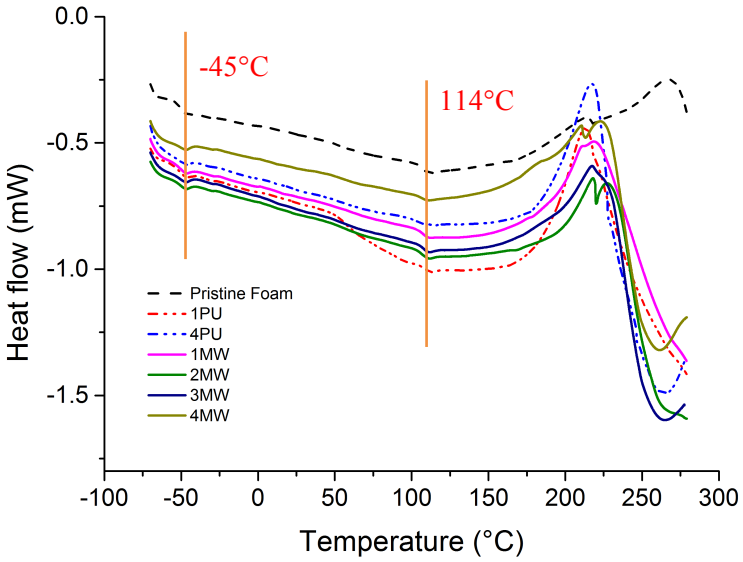

Fig. 10. DSC analysis of pristine and multilayer coated foams.

4. Conclusions

The paper has described a simple and scalable method to fabricate multilayer PU foams coated with CNT inks. This simple dip-coating technique contributed to a formation of a microarchitecture on the foam skeleton similar to the multilayer sandwich covering in each cell foam rib. The highly entangled MWNTs represent the core of this sandwich, and water-based PUD as the external skins. The global significant increase in damping and energy dissipation in these foams is provided by the nanotube-nanotube interfacial sliding damping mechanism within the core layer. The electrical conductivity of the ink layer was also measured to assess the surface coating coverage, and with 0.1wt% of MWNT ink concentration full coverage was achieved with electrical conductivity of the foam increasing dramatically to ~1 S/m. The microarchitectured foam nanocomposites show significant increments in terms of both the elastic modulus and the loss factor, with an optimal performance achieved with up to two layers of coating. The use of increased numbers of layers produced a drop of the loss factor because of the substantial augmentation of the storage modulus. Nomogram obtained from DMA tests were also reported for the coating layer selection guidance regarding the foam operating frequency and the desired elastic modulus for damping.

ACKNOWLEDGEMENTS

The authors acknowledge Thomas Swan & Co. Ltd., UK for funding this project and supplying the CNTs.

REFERENCES

[1] V. Dolomanova, J.C.M. Rauhe, L.R. Jensen, R. Pyrz, A.B. Timmons, Mechanical properties and morphology of nano-reinforced rigid PU foam, J Cell Plast 47(1) (2011) 81-93.

[2] M.T. Chen, L. Zhang, S.S. Duan, S.L. Jing, H. Jiang, M.F. Luo, C.Z. Li, Highly conductive and flexible polymer composites with improved mechanical and electromagnetic interference shielding performances, Nanoscale 6(7) (2014) 3796-3803.

[3] L.M. Chen, L.S. Schadler, R. Ozisik, An experimental and theoretical investigation of the compressive properties of multi-walled carbon nanotube/poly(methyl methacrylate) nanocomposite foams, Polymer 52(13) (2011) 2899-2909.

[4] N. Athanasopoulos, A. Baltopoulos, M. Matzakou, A. Vavouliotis, V. Kostopoulos, Electrical conductivity of polyurethane/MWCNT nanocomposite foams, Polym Composite 33(8) (2012) 1302-1312.

[5] K. Dai, X. Ji, Z.D. Xiang, W.Q. Zhang, J.H. Tang, Z.M. Li, Electrical Properties of an Ultralight Conductive Carbon Nanotube/Polymer Composite Foam Upon Compression, Polym-Plast Technol 51(3) (2012) 304-306.

[6] R. Verdejo, R. Stämpfli, M. Alvarez-Lainez, S. Mourad, M.A. Rodriguez-Perez, P.A. Brühwiler, M. Shaffer, Enhanced acoustic damping in flexible polyurethane foams filled with carbon nanotubes, Compos Sci Technol 69(10) (2009) 1564-1569.

[7] J. Lee, G.H. Kim, C.S. Ha, Sound Absorption Properties of Polyurethane/Nano-Silica Nanocomposite Foams, J Appl Polym Sci 123(4) (2012) 2384-2390.

[8] C.H. Sung, K.S. Lee, K.S. Lee, S.M. Oh, J.H. Kim, M.S. Kim, R.M. Jeong, Sound damping of a polyurethane foam nanocomposite, Macromol Res 15(5) (2007) 443-448.

[9] M. Bandarian, A. Shojaei, A.M. Rashidi, Thermal, mechanical and acoustic damping properties of flexible open-cell polyurethane/multi-walled carbon nanotube foams: effect of surface functionality of nanotubes, Polym Int 60(3) (2011) 475-482.

[10] Y.B. Wang, G.A. Sotzing, R.A. Weiss, Conductive polymer foams as sensors for volatile amines, Chemistry of Materials 15(2) (2003) 375-377.

[11] Y.J. Chen, Y. Li, B.T.T. Chu, I.T. Kuo, M.C. Yip, N. Tai, Porous composites coated with hybrid nano carbon materials perform excellent electromagnetic interference shielding, Compos Part B-Eng 70 (2015) 231-237.

[12] X.C. Zhang, H.X. Peng, A.P. Limmack, F. Scarpa, Viscoelastic damping behaviour of cup stacked carbon nanotube modified epoxy nanocomposites with tailored interfacial condition and re-agglomeration, Compos Sci Technol 105 (2014) 66-72.
[13] L.Y. Sun, R.F. Gibson, F. Gordaninejad, J. Suhr, Energy absorption capability of nanocomposites: A review, Compos Sci Technol 69(14) (2009) 2392-2409.
[14] X.C. Zhang, F. Scarpa, R. McHale, H.X. Peng, Poly(methyl methacrylate)-decorated single wall carbon nanotube/epoxy nanocomposites with re-agglomeration networks: Rheology and viscoelastic damping performance, Polymer 87 (2016) 236-245.
[15] R.M. Lin, C. Lu, Modeling of interfacial friction damping of carbon nanotube-based nanocomposites, Mech Syst Signal Pr 24(8) (2010) 2996-3012.
[16] K. Liang, S.Q. Shi, Soy-based Polyurethane Foam Reinforced with Carbon Nanotubes, Key Eng Mat 419-420 (2010) 477-480.
[17] H.B. Yao, J. Ge, C.F. Wang, X. Wang, W. Hu, Z.J. Zheng, Y. Ni, S.H. Yu, A Flexible and Highly Pressure-Sensitive Graphene-Polyurethane Sponge Based on Fractured Microstructure Design, Advanced Materials 25(46) (2013) 6692-6698.
[18] S. Chun, A. Hong, Y. Choi, C. Ha, W. Park, A tactile sensor using a conductive graphene-sponge composite, Nanoscale (2016).
[19] D.C. Corporation, Isopropanol Technical Data Sheet, Form No. 327-00031-0812, Dow Corning Technical Data Sheet (2012).
[20] N.B. Vargaftik, B.N. Volkov, L.D. Voljak, International Tables of the Surface-Tension of Water, J Phys Chem Ref Data 12(3) (1983) 817-820.
[21] A.B. GmbH, ALBERDINGK Water-based Polyurethane and Acrylate Dispersions Technical Data Technical Data (2013).
[22] D.Y. Zhang, F. Scarpa, Y.H. Ma, K. Boba, J. Hong, H.W. Lu, Compression mechanics of nickel-based superalloy metal rubber, Mat Sci Eng a-Struct 580 (2013) 305-312.
[23] D. Zhang, F. Scarpa, Y. Ma, J. Hong, Y. Mahadik, Dynamic mechanical behavior of nickel-based superalloy metal rubber, Materials & Design 56 (2014) 69-77.
[24] M. Bianchi, F. Scarpa, Vibration transmissibility and damping behaviour for auxetic and conventional foams under linear and nonlinear regimes, Smart Mater Struct 22(8) (2013).
[25] M.L. Williams, R.F. Landel, J.D. Ferry, Mechanical Properties of Substances of High Molecular Weight .19. The Temperature Dependence of Relaxation Mechanisms in Amorphous Polymers and Other Glass-Forming Liquids, Journal of the American Chemical Society 77(14) (1955) 3701-3707.

[26] G.L. Wilkes, Introduction to Polymer Viscoelasticity, 2nd Edition - Aklonis,Jj, Macknight,Wj, Journal of the American Chemical Society 106(4) (1984) 1176-1176.
[27] K.P. Menard, Dynamic mechanical analysis : a practical introduction, CRC Press, Boca Raton, FL, 2008.
[28] M.L. Hobbs, K.L. Erickson, T.Y. Chu, Modeling decomposition of unconfined rigid polyurethane foam, Polym Degrad Stabil 69(1) (2000) 47-66.